Selective H 2 S Absorption in Aqueous Tertiary Alkanolamine Solvents: Experimental Measurements and Quantitative Kinetic Model

Xavier Rozanska, Alain Valtz, Mauro Riva, Christophe Coquelet, Erich Wimmer, Karen Gonzalez-Tovar, Frédérick de Meyer

Selective H_2S Absorption in Aqueous Tertiary AlkanolAmine Solvents: Experimental Measurements and Quantitative Kinetic Model

Xavier Rozanska[§], Alain Valtz[‡], Mauro Riva[‡], Christophe Coquelet[‡], Erich Wimmer[§], Karen Gonzalez-Tovar[†], Frédérick de Meyer[†‡]*

§ Materials Design SARL, 42 Avenue Verdier, 92120 Montrouge, France

† TotalEnergies S.E., OneTech, Gas & Low Carbon, Acid Gas Entity, CO_2 & Sustainability R&D Program, Paris, 92078 France

‡ MINES Paris, PSL University, Center of Thermodynamics of Processes, 35 rue St Honoré, 77300 Fontainebleau, France

*frederick.de-meyer@totalenergies.com

Keywords: gas treatment, hydrogen sulfide, carbon dioxide, kinetics, molecular model, selective absorption

ABSTRACT

In the treatment of many fuel gases such as biogas, natural gas, syngas, and so on, tertiary alkanolamines play an important role in the selective removal of H_2S with respect to CO_2. The selectivity might be required for various reasons: to respect more stringent H_2S specifications, to optimize the performance of the Claus unit, to lower the cost of CO_2 capture, and so on. The

H_2S/CO_2 selectivity is mainly kinetic, and, to a lesser extent, thermodynamic. A novel experimental set-up has been put in place to measure the time-evolution of the simultaneous absorption of H_2S and CO_2. The results of an extensive experimental campaign with 18 different aqueous tertiary alkanolamine solvents (13%mol. amine, 87%mol. H_2O) are presented. Although the absorption of H_2S is expected to be a very fast proton transfer, a significant variation in H_2S absorption rates, and thus in selectivity is observed. This could not only be explained by the pK_a or the viscosity of the amines. Therefore, an accurate quantitative molecular simulations-based kinetic model is developed and validated. The study allowed to better understand the molecular origin of selectivity, as well as to identify amines with a higher selectivity than aqueous MDEA (MethylDiEthanolAmine), the standard industrial selective solvent.

INTRODUCTION

Biogas offers promising prospects for the energy transition and can be used for electricity generation, injection into the existing natural gas grids as well as mobility applications. Depending on the source of biogas, this green gas obtained by fermentation contains mainly CH_4 (35-70 mol%) and CO_2 (15-50 mol%), but also undesirable compounds such as H_2S (0 to 2 mol%), H_2O (0 to 10 mol%), NH_3, O_2, N_2, and siloxanes [1]. Those compounds need to be separated from the methane for safety and operational reasons, and to increase the calorific value of the gas. The biogas (methane) specifications vary but are commonly around < 4 ppm H_2S and < 2.5 v% CO_2. Biogas treatment typically occurs in two steps: a biogas cleaning step followed by an upgrading. Many industrial solutions exist for each step, and, when looking at the overall process, the optimal choice depends on many factors like the capacity, the exact gas composition, thermal integration, the cost of utilities, operational costs, acceptable methane losses, compression pressure of the biomethane, and so on [1], [2]. For plants with higher

capacities (> 3000 N m^3 hr^{-1}) amine scrubbing is often used for CO_2 and H_2S removal. Amine scrubbing shows very low methane losses and a high purity CO_2 production and allows for the simultaneous removal of H_2S, NH_3, and CO_2. Because the acid gas treatment takes place at atmospheric pressure it is, however, challenging to reach the H_2S specifications of 4 ppm with solely amine scrubbing. Therefore, a second desulphurization step is required, e.g., using activated carbon and/or biological desulphurization. The overall process might be improved with the development of more selective and better-performing amine solvents.

Contrary to biogas treatment, natural gas sweetening takes place at much higher pressures (40 to 70 bar). Natural gas can contain significant amounts of acid gas (typically 0-30 v% CO_2, 0-30 v% H_2S) but the specifications of treated natural gas are very similar to biogas (around 4ppm H_2S, and 50 ppm or 2.0-2.5 v% CO_2 for LNG or pipeline, respectively) and can be reached with solely an amine scrubber, thanks to the high operating pressure of the absorption column. To simultaneously respect the asymmetrical H_2S (<4 ppm) and CO_2 (< 2.0-2.5 v%) specification a selective solvent can be used that preferentially absorbs H_2S over CO_2 [3]. Techno-economic studies have shown that a further increase of the selectivity might lower the cost of CO_2 capture from natural gas containing H_2S [4], [5].

Low-pressure selective absorption is also applied in the natural gas industry, for example, in the acid gas enrichment (AGE) unit or the tail gas treatment unit (TGTU), in the upstream and downstream Claus sulfur recovery units, respectively. The main driving forces to improve the selectivity of the solvents in both TGTU and AGE are the reduction of CO_2 emissions, Claus unit optimization (only for AGE), and lower SO_2 emissions. Other applications of selective H_2S removal are the treatment of syngas, coke oven gas, landfill gas, refinery gas, and so on.

A recent exhaustive review on H_2S removal is available in [6]. In the current work the focus is on solvents. Physical solvents can be used for bulk selective H_2S removal. Many molecules can be used [4], [7], [8], and common examples are the Rectisol, Purisol, and Selexol processes. The selectivity is thermodynamic [9].

Tertiary amines such as methyldiethanolamine (MDEA) and sterically amines [10] such as 2-amino-2-methyl-1-propanol (AMP) are well known selective amines, with MDEA the most common in the industry [3], [11], [6]. Sterically hindered ethoxyethanol amines are also used industrially, and Lu et al. studied a blend of a tertiary sterically hindered ethoxyethanolamine (2-tertiarybutylamino-2-ethoxyethanol (TBEE)) with MDEA [12]. Blends of sterically hindered 2-(tert-butylamino)ethanol (TBE) and AMP have been shown to be selective towards H_2S absorption [13], [14]. The selectivity of chemical absorption is both thermodynamic and kinetic, with the kinetic factor being the dominant contributor [15]. Indeed, the chemical absorption of H_2S is a very fast proton transfer, $H_2S+MDEA \leftrightarrow HS^- + MDEAH^+$, while the absorption of CO_2 is a much slower reaction: $CO_2+H_2O+MDEA \leftrightarrow HCO3^-+MDEAH^+$.

Process models of acid gas absorption in aqueous MDEA consider that CO_2 is limited by the mass transfer in the liquid phase, while the absorption of H_2S is limited by the mass transfer in the gas phase [16] [17]. This is important, as it restricts the possibilities to further improve the selectivity. The model equations of the rates at the gas-liquid interface are then different for CO_2 and H_2S. The equation for CO_2 is [18]:

$$D_{CO_2}\frac{d^2C_{CO_2}}{dx^2} = r \qquad \text{Eq. 1}$$

because the rate of the reaction is considered slow, and the reaction is consequently assumed to be limited by the mass transfer. In Eq. 1, C_{CO2} is the CO_2 concentration in the solvent, D_{CO2} is the diffusivity of CO_2 in the solvent and r is the reaction rate. The equation for H_2S is [18]:

$$D_{H_2S}\frac{d^2C_{H_2S}}{dx^2} = D_{amine}\frac{d^2C_{amine}}{dx^2} \quad \text{Eq. 2}$$

because the rate of the reaction of absorption of H_2S is fast and the transfer is limited by the diffusivity. According to the double film theory of Whitmann [19], the mass transfer rate (N_A) is proportional to the liquid mass transfer coefficient, K_L, the interfacial area a, and the gradient of concentration of solute from the gas liquid interface, C_i, and the liquid. Considering the gas phase, the mass transfer rate is proportional to gas mass transfer coefficient, K_G and the gradient of pressure from gas phase to gas liquid interface P_i:

$$N_A = K_L a(C_i - C) = K_G a(P - P_i) \quad \text{Eq. 3}$$

To improve the selectivity one can improve the mass transfer in the gas phase, for example using a rotating packed bed reactor [20], [21] but this should certainly also improve the mass transfer in the liquid phase (CO_2 absorption), potentially even decreasing the selectivity. Another possibility is to slow down the mass transfer of CO_2 in the liquid phase, for example, by operating at lower temperatures, by using less reactive amines, or by replacing part of the water with certain physical co-solvents [22]. The latter two options, however, might also negatively impact the H_2S absorption kinetics and capacity [23], [24], [25], making it harder to reach the H_2S specification in the treated gas [24] and thus limiting or even canceling the potential gain in selectivity at iso-H_2S absorption. The addition of small quantities of acids (and a further increase in solvent flow rate) might allow reaching a lower H_2S content in the treated gas [26]. Acids

slightly negatively impact the mass transfer and absorption capacity, but they also destabilize the HS^- and HCO_3^- ions, and, consequently, the regenerated solvent is leaner, resulting in better H_2S absorption on the top of the absorption column. This is mainly true at low pressure.

To optimize the aqueous tertiary amines chemical solvents for selective absorption of CO_2 and H_2S from gases, a better quantitative kinetic model of acid gas absorption would be beneficial. The thermodynamic CO_2 absorption capacity, and, to a much lesser extent, the CO_2 absorption rates, have been measured experimentally for a wide range of tertiary amines [27], [28], [29]. Rozanska et al. recently developed a molecular simulations-based quantitative kinetic model for the absorption of CO_2 in aqueous tertiary amines [30], and Orlov et al. subsequently built on this model to develop a tool to perform a virtual screening of thousands of tertiary amines to identify better candidates for CO_2 removal [31]. As pointed out in a recent review on H_2S removal, there are, however, no systematic experimental studies available in the literature covering the simultaneous H_2S and CO_2 absorption, and thus, the selectivity, for a wide range of (tertiary) amines [6].

In this paper, the results are presented of a novel experimental set-up to simultaneously measure the simultaneous H_2S and CO_2 absorption rates in several aqueous tertiary alkanolamine solvents. Subsequently, the molecular simulations-based model of CO_2 absorption Rozanska et al. [30] is extended to the absorption rate of H_2S and the kinetic H_2S/CO_2 selectivity.

METHODS

Experimental Measurements

To measure the kinetics of simultaneous absorption or desorption of CO_2 and H_2S in aqueous amine solutions, a thermo-regulated constant interfacial area Lewis-type reactor cell was used

[32]. The principle of the method is based on pressure decay. We follow the decrease of the pressure of each acid gas with time. The transfer rate can be expressed by considering the gas phase as ideal and the concentration of solute in the bulk liquid to be very small compared to its concentration at the interface. No resistance in the gas phase for mass transfer is considered. One can show that [32]:

$$N_A = \frac{-V_g}{RT}\frac{dP_g}{dt}, \qquad \text{Eq. 4}$$

where V_g is the volume of the gas phase. Eq. 4 recalls the expression of the rate of transfer in Eq. *3*.

The reactor is equipped with an internal stirring system (magnetic stirrer) with an external motor (see Supplementary Information). The operator needs to take care to select the speed of stirring without disturbing the interface (the interface must be flat). Temperature and temperature gradient are given by two platinum probes located at the upper and lower flanges. The cell is immersed in a liquid bath. An electric resistor is introduced into the upper flange to control the gradient of temperature and avoid condensation of water and amine in the connection between the cell and the pressure transducer. To determine the partial pressures of the acid gases, it is necessary to measure the vapor phase composition. Two capillary samplers are adapted to sample the vapor phase. The capillary samplers (ROLSI®) can withdraw and send micro samples to a gas chromatograph without perturbing the equilibrium conditions over numerous samplings, thus leading to repeatable and reliable results. Analytical work was carried out using a gas chromatograph (Perichrom model PR2100, France) equipped with two thermal conductivity detectors (TCD) connected to a data software system. Helium is used as the carrier gas in this experiment. The model of the gas chromatograph (GC) column is Porapak R (Porapak

R 80 / 100 mesh, 1 m x 2 mm ID Silcosteel). Each ROLSI® sampler is connected to a TCD. The ROLSI® samplers permit to take more samples of the vapor phase during the absorption process to determine more acid gas partial pressures, which permits to better evaluate the rates of absorption. A tube allows either to evacuate or to introduce CO_2 and H_2S from or into the cell. A computer equipped with data acquisition system records the pressure as a function of time.

The experimental procedure is the following:

- The desired amount of solvent is introduced into the cell. The density obtained using a low-pressure vibrating tube densitometer (Anton Paar DSA 5000) is used to determine the exact number of moles of solvent.
- The speed of stirring is selected. Through visual inspection, it is confirmed that the surface of the liquid is flat.
- At least 5 bar of methane is added. It is added to permit the sampling to the GC, which is otherwise impossible when the pressure is lower than the GC carrier gas pressure.
- Acid gases are added from the thermal press. We record pressure and temperature before and after the loading. This protocol permits to calculate very accurately the number of moles of acid gases that are introduced.

During the absorption of the acid gases, we take samples to follow the evolution of the vapor composition as a function of time (through the CO_2 and H_2S partial pressures). When the equilibrium is reached, the vapor phase composition is determined. We assumed that the equilibrium is reached when there are no variations of the pressure and temperature for at least 5 min at any speed of stirring. The determination of the solubility of CO_2 or H_2S at the equilibrium

is the same as in [33]. More details concerning the method are presented in the Supplementary Information.

We used the GERG 2008 Equation of state [34] implemented in REFPROP 10.0 [35] to estimate the densities of the vapor phase, which is a mixture of CO_2, H_2S and CH_4, because it predicts densities with high accuracy.

The calculation of the acid gas solubility in the solvent is based on mass balance and is described below.

The volume of liquid phase (V^{L}) is obtained by considering the number of moles of solvent introduced (n_{solvent}) and the density of the solvent at the temperature of measurement in the cell ($\rho(T_{\mathrm{cell}})$):

$$V^{\mathrm{L}} = \frac{n_{\mathrm{solvent}}}{\rho(T_{\mathrm{cell}})} \qquad \text{Eq. 5}$$

Consequently, the volume of the vapor phase (V^{V}) is calculated by difference from the total volume (V^{T}) and the volume of the liquid phase:

$$V^{\mathrm{V}} = V^{\mathrm{T}} - V^{\mathrm{L}} \qquad \text{Eq. 6}$$

If the introduction of the solute does not modify the level of the liquid interface in the equilibrium cell, we can consider that:

$$V^{\mathrm{L}} = \pi r_{\mathrm{cell}}^2 h_{\mathrm{liq}} \qquad \text{Eq. 7}$$

where r_{cell} is the radius of the equilibrium cell and h_{liq} the level of the vapor-liquid interface.

The number of moles of solute in the vapor phase is calculated by considering the density of the gas at the temperature and pressure of solute ($P_{\mathrm{solute}} = P_{\mathrm{cell}} - P_{\mathrm{solvent}}^{\mathrm{sat}}$). REFPROP v10.0 is

used to calculate this density $\rho^{\mathrm{V}}(T_{\mathrm{cell}}, P_{\mathrm{solute}})$. In case of a mixture, the global composition needs to be considered $\rho^{\mathrm{V}}(T_{\mathrm{cell}}, P_{\mathrm{solute}}, y)$.

The number of moles of solute in the vapor phase (n^{V}) is:

$$n^{\mathrm{V}} = V^{\mathrm{V}}\rho^{\mathrm{V}}(T_{\mathrm{cell}}, P_{\mathrm{solute}}) \qquad \text{Eq. 8}$$

For the mixture, the same equation is used to calculate the total number of moles of solute in the vapor phase.

The number of moles of solute in the liquid phase is determined from:

$$n^{\mathrm{L}} = n^{\mathrm{T}} - n^{\mathrm{V}} \qquad \text{Eq. 9}$$

In case of mixture, the number of moles in the liquid phase of each species *i*, where *i* is CH_4, H_2S, or CO_2, is calculated from:

$$n_i^{\mathrm{L}} = z_i n^{\mathrm{T}} - y_i n^{\mathrm{V}} \qquad \text{Eq. 10}$$

where *z* is the global composition of the mixture and *y* the composition of the vapor phase.

The solubility is determined from:

$$\mathrm{x}_i = \frac{n_i}{\sum_{i=1}^{j} n_j} \qquad \text{Eq. 11}$$

This experimental protocol permits to measure individually the CO_2 and H_2S composition in the different phases as a function of time. Consequently, it is possible to evaluate the CO_2/H_2S absorption selectivity at the thermodynamic equilibrium as well as at any time during the process.

Model simulations based model and computational details

The approach described in Rozanska *et al*. [30] was used to calculate the rates of CO_2 absorption in aqueous tertiary amine solvents, which depend primarily on the solvation properties of OH^-, CO_2, and HCO_3. The rate is given by:

$$R_{\mathrm{MD}} = A(T) \times \exp\left(\frac{-\Delta G^{\neq}}{RT}\right) \times [\mathrm{CO_2}][\mathrm{OH^-}] \qquad \text{Eq. 12}$$

where R_{MD} is the absorption rate of CO_2, $[CO_2]$ and $[OH^-]$ are the concentrations in the liquid phase of carbon dioxide molecules and hydroxyl anions, respectively, $\Delta G^{\ddagger}$ is the Gibbs free energy barrier of the reaction CO_2 + OH^- to HCO_3^-, RT is the macroscopic thermodynamic energy unit, where R is the universal gas constant, T is the absolute temperature, and $A(T)$ is a temperature-dependent pre-exponential factor.

Is it possible to make a parallel between Eq. 12 and the Hatta theory applied to acid gas absorption [36]. A chemical reaction in a liquid phase will enhance the absorption of the acid gas. The Hatta number is given by [37]:

$$Ha = \frac{\sqrt{kC_{\mathrm{amine}}D_A}}{K_L} \qquad \text{Eq. 13}$$

where k is the kinetic constant of the reaction, C_{amine} the concentration of amine, and D_A the diffusion coefficient of the solute (i.e., the acid gas) in the liquid phase. When a chemical reaction occurs in the liquid phase, the rate of absorption in Eq. 3 can be expressed as:

$$N_A = K_L a \mathrm{E}(C_i - C) \qquad \text{Eq. 14}$$

where E is the ratio of the rates of absorption with and without chemical reaction. The magnitude of the enhancement factor E depends on the value of Hatta number. Considering our application,

as the quantity of dissolved acid is very low (condition of initial kinetics), we can consider that the pseudo-first order regime is applied. For CO2, the rate of absorption is given by:

$$N_A = a[\mathrm{CO_2}]\sqrt{kC_{amine}D_A} \approx K_L aHa[\mathrm{CO_2}] \quad \text{Eq. 15}$$

This equation is closely related to Eq. 12. In the condition of initial kinetics and at low acid gas absorption loading, the concentration of solvated hydroxyl, $[\mathrm{OH^-}]$, is nearly constant because it is restored from the unreacted amine. From Eq. 15, we can observe that the rate of absorption is dependent on the kinetic constant (Hatta number) and diffusion coefficient (liquid mass transfer coefficient (K_L).

In Eq. 12, $\Delta G^{\ddagger}$ is obtained from the differences in the total energies of OH^- + CO_2 and HCO_3^- in the aqueous amine solvents calculated in molecular dynamics simulations, and an Evans-Polanyi relation [38], $[CO_2][OH^-]$ is obtained numerically by solving the pH equations, and $A(T)$ is fitted using the experimental rates of the reaction CO_2 + OH^- in 10 aqueous amine solvents. The Evans-Polanyi relation between $\Delta G^{\ddagger}$ and the energy differences of solvation of OH^- + CO_2 and HCO_3^- is:

$$\Delta G^{\ddagger} = a\,\Delta E(T) + b \quad \text{Eq. 16}$$

where a and b are fitted to reproduce the experimental rates in pure water and 10 aqueous amine solvents and $\Delta E(T)$ is the energy difference of solvation of OH^- + CO_2 and HCO_3^- obtained from molecular dynamics simulations using LAMMPS as described above. Additional details and the values for $A(T)$, a, and b can be found in Rozanska *et al*. [30].

A similar approach was followed for H_2S. The relation between the energies of $H_2S + OH^-$ and $SH^- + H_2O$ solvated in the aqueous amine solvents and the rate of absorption of H_2S is discussed in the Results section.

The total energies of the aqueous amine solvents, with and without solvated H_2S, CO_2, OH^-, SH^-, and HCO_3^- were evaluated by classical molecular mechanics (MM) dynamics simulations [39] using the Large-scale Atomic/Molecular Massively Parallel Simulator software (LAMMPS) [40] with the Extended Polymer Consistent Force Field (PCFF+) [41] [42] [43] as implemented in *MedeA* 3.4 [44]. The non-bonded energy terms were evaluated within a cutoff distance of 9.5 Å. Beyond the cutoff distance, the particle-particle-particle-mesh (PPPM) [45] method was used for the Coulomb interactions, while a tail correction is applied for the van der Waals interactions [46]. Temperature and pressure were controlled using the Nosé-Hoover thermostat [47] and barostat [39], respectively. The time step for the integration of the Newtonian equation of motion [48] was set to 0.2 fs. The compositions of the atomistic models of the aqueous amine solvents in the MM simulations reflect the experimental ones. All experimental aqueous amine solvents have a concentration of 13% mol. amine and 87% mol. H_2O. The unit cells contain 25 amine and 168 H_2O molecules. They are cubic with dimensions larger than twice the cutoff distance of 9.5 Å, namely, between 22 and 26 Å. The initial configurations, with imposed periodic boundary conditions and a density set to 0.7 g L^{-1}, were generated using the Amorphous Materials Builder module [44], which employs a Monte Carlo approach that samples the translational, rotational, and conformational degrees of freedom of the component species to generate realistic configurations of atomistic models. Once the models were generated, they were equilibrated at T= 363.15 K for 1.5 ns of simulation in the isothermal-isochoric (NVT) ensemble before equilibration in the isothermal-isobaric (NPT) ensemble at P=1 atm with a fluctuating

temperature from 363.15 to 323.15 K for 1 ns. Next, the systems were further relaxed for 0.5 ns in the NPT ensemble at P=1 atm and T=323.15 K. Following this equilibration procedure, an NPT simulation was performed at P=1 atm and T=323.15 K for 5 ns to determine the average density of each system (Table S1).

Other properties were analyzed using molecular dynamics simulations: the models and methods are described in the Supporting Information.

After the 5 ns molecular mechanics simulation in the NPT ensemble of each aqueous amine solvent, the final structure is collected and duplicated: in the first duplicate, OH^- and CO_2 or OH^- and H_2S are inserted into the cell, and, in the second duplicate, HCO_3^- or H_2O and SH^- are added, respectively. OH^-, CO_2, H_2S, HCO_3^-, and SH were initially placed surrounded by water molecules in the cells. The densities of the modified systems are set to the average value obtained from the 5 ns NPT simulation of aqueous amine solvent in the absence of OH^- and CO_2, or HCO_3^-. Because the reactant (OH^-+CO_2 or OH^-+H_2S) has the same mass as the product (HCO_3^- or SH^-+H_2O, respectively)$^-$, the volumes of the cell of aqueous amine with the reactants and the products of a reaction are identical. The total energies of all aqueous amine solvents, with and without solvated CO_2, OH^-, H_2S, SH^-, and HCO_3^- were evaluated from simulations in the NVT ensemble at T=323.15 K. The systems were first equilibrated for 4 ns. The energies were then sampled over a series of 12×5 ns NVT runs. The sampling time to get a reaction energy value in a solvent is thus 120 ns.

RESULTS

A set of 18 aqueous amine solvents is selected based on their relevance, chemical diversity, and availability (Table 1).

Table 1. Amines in the selected aqueous amine solvents and their pK_a.[a]

Amine			pK_a	
Label	Name	CAS Number	Exp.	Pred.
MDIPA	N-methyldiisopropanolamine	4402-30-6		8.75
HAP	N,N-bis(2-hydroxyethyl)isopropanolamine	6712-98-7		8.43
DEA-12-PD	3-(Diethylamino)-1,2-propanediol	621-56-7	9.89	9.67
DEAE-EO	2-(2-Diethylaminoethoxy)ethanol	140-82-9		9.43
EDEA	N-ethyldiethanolamine	139-87-7	8.86	8.51
EPOL	1-Ethyl-3-pyrrolidinol	30727-14-1		10.37
DMAEE	2-[2-(Dimethylamino)ethoxy]ethanol	1704-62-7		9.13
MDEA	1-Methyl-4-piperidinemethanol	105-59-9	8.65	8.41
MPM	1-Methyl-4-piperidinemethanol	20691-89-8		9.17
1MPOL	1-Methyl-3-pyrrolidinol	13220-33-2		10.49
HMP	N-Methyl-4-piperidinol	106-52-5		9.53
3H-1MPP	N-Methyl-3-piperidinol	3554-74-3	8.94	8.89
NMM	4-Methylmorpholine	109-02-4		8.18
THEE	N,N,N',N'-Tetrakis(2-hydroxyethyl)ethylenediamine	140-07-8		7.92
TEA	Triethanolamine	102-71-6	7.85	8.09
THPE	N,N,N',N'-Tetrakis(2-hydroxypropyl)ethylenediamine	102-60-3		8.65
1E-3HPP	1-Ethyl-3-hydroxypiperidine	13444-24-1	9.21	9.70
3PP-12-PD	3-piperidino-1,2-propanediol	4847-93-2	9.49	9.88

[a]The experimental and predicted pK_a are from Chowdhury *et al*. [28] and Mansouri *et al*. [49], respectively. A discussion on accuracy of pK_a can be found in [50].

The rates of absorption of H_2S and CO_2 were measured for each solvent. The procedure for deriving the rates of absorption of CO_2 and H_2S in the aqueous amine solvents from the raw experimental measurements and the uncertainties on the rates are described in the Supporting Information, where all numerical values are also reported (Tables S1, S2, and S3). The data are summarized in **Figure 1**.

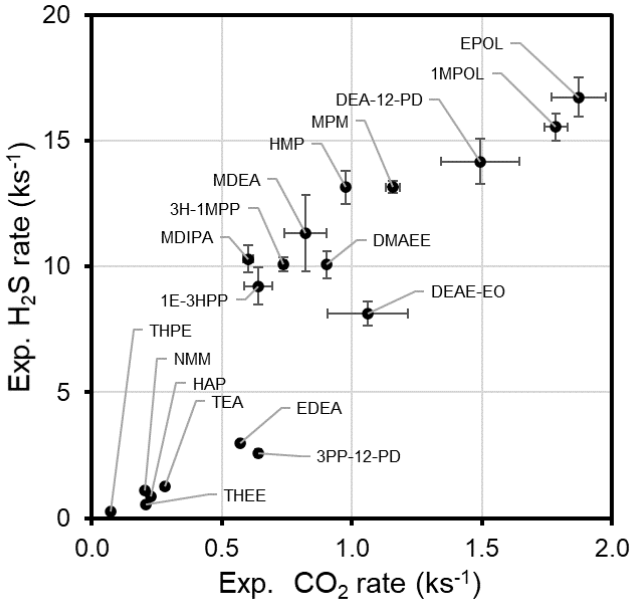

Figure 1. Experimental rates of absorption of CO_2 and H_2S at T=323.15 K in the aqueous amine solvents (13%mol. amine, 87%mol. H_2O).

There is a weak linear correlation between the CO_2 and H_2S absorption rates (**Figure 1**). There is a break in this linear relationship around r_{CO2}=0.6 ks^{-1}, resulting in two subsets of amine solvents that show stronger linear relationships between the rates of CO_2 and H_2S. The first subset includes the aqueous THPE, NMM, HAP, THEE, EDEA, and 3PP-12-PD solvents, and the

second subset includes the other aqueous amine solvents. However, there are still large differences between the rates of absorption in the different aqueous amine solvents. The reason for this behavior is unclear. It might be that for the first set the H_2S absorption is limited by liquid-phase mass transfer, while for the second subset H_2S absorption is limited by gas-phase mass transfer. The pK_as of the amines (Table 1) impacts the rate of absorption. However, it has been observed that the pK_a plays only a modest role in the rates of absorption of CO_2 in aqueous amine solvents [30]. It appears that the same is true for the rates of absorption of H_2S. The coefficients of determination (R^2) of the linear fits between the pK_a of the amines and the rates of absorption of CO_2 and H_2S in the aqueous amine solvents are 0.69 and 0.51, respectively. The correlation between H_2S absorption rates and viscosities of the solvents was also analyzed. Although a very high viscosity resulted in low absorption rates, there is no correlation between experimental viscosity of the solvents and absorption rates of CO_2 and H_2S (Supplementary Information).

Another way to analyze the correlation between the rates of CO_2 and H_2S and the pK_a of the amines is to report the selectivity of absorption of H_2S vs. CO_2, which is the ratio of the H_2S rate to the CO_2 rate (**Figure 2**). The variation of the H_2S/CO_2 selectivity as a function of the rate of H_2S has a volcano shape. However, the dispersion of the values at the maximum H_2S/CO_2 selectivity, around an H_2S rate of 10 ks^{-1}, is very large: the selectivity goes from 7 to 17 in the range of H_2S rate between 8 and 12 ks^{-1}. Aqueous MDEA, the industrial reference, shows one of the best selectivity. Aqueous MDIPA is found to have a higher selectivity towards H_2S than aqueous MDEA. The absorption rate of H_2S in both solvents is similar. This result is not surprising, as MDIPA is very similar to MDEA, the only difference being the two methyl groups, making the molecule more hydrophobic and adding some steric hindrance, two effects that

increase the selectivity towards H_2S. Note that the slightly higher hydrophobicity will result in more undesirable CH_4 co-absorption. Interestingly, DEAE-EO, an ethoxyethanolamine shows a much lower selectivity with respect to MDEA, suggesting that the addition of an ether group doesn't favor selectivity. Amines with either a very low or a very high H_2S absorption rate also tend to be less selective.

To better understand these variations, we develop a model based on values obtained from atomistic simulations. Such a model already exists for the rate of absorption of CO_2 [30]. Here, we focus on the rate of absorption of H_2S.

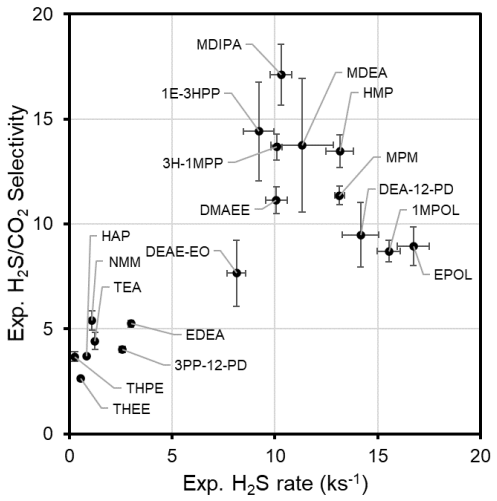

Figure 2. Experimental selectivity of absorption of H_2S over CO_2 as a function of the rate of absorption of CO_2 and H_2S at T=323.15 K in the aqueous amine solvents (13%mol. amine, 87%mol. H_2O).

As mentioned in the introduction, process models usually assume that the rates of absorption of CO_2 and H_2S are limited by respectively liquid and gas phase mass transfer [16], [17]. The measured experimental rates of absorption of H_2S are about one order of magnitude larger than those of CO_2, strongly suggesting that the diffusion limits for CO_2 and H_2S are different and

affect the absorption rates (**Figure 1**). Therefore, we computed the diffusion constants of CO_2, H_2S, and amine in a selection of aqueous amine solvents using atomistic simulations and analyzed their correlations with the measured experimental rates of absorption of H_2S (Supporting Information, Figures S3, S4, and S5). No correlations were found between the calculated diffusion constants and the measured experimental rates. Furthermore, it is reported that the absorption rate of H_2S is so fast that the rate-determining step is related to the phenomenon occurring at the interface between the liquid and the gas phases [16], [17]. To verify this, we computed the surface tension at the interface between the aqueous amine solvents and the gas phase (Supporting Information, Figure S6). No correlation was found between the computed surface tension and the measured experimental rates. Second, if the absorption of H_2S is controlled by a chemical reaction, there is no a priori reason why the rate-determining steps in the absorption of CO_2 and H_2S should be the same. There are several elementary reaction mechanisms involved in the absorption of H_2S. Only one is the rate-determining step, while several kinetic steps may compete. To determine which step is the rate-determining step, we computed several reaction energies for a selection of aqueous amine solvents and analyzed their correlations with the experimental rates of H_2S absorption (Supporting Information, Figures S7, S8, and S9). The strongest correlation between the calculated data and the experimental rate values is obtained with the reaction energy of:

$$H_2S_{(solv)} + OH^-_{(solv)} \rightarrow SH^-_{(solv)} + H_2O_{(solv)} \quad \text{Eq. 17}$$

where the solvent (solv) is an aqueous amine solvent, using a logarithmic relationship:

$$\log\left(r_{\mathrm{H2S,model}}\right) = A\Delta E_{\mathrm{H2S}} + \mathrm{B} \quad \text{Eq. 18}$$

where ΔE_{H2S} is the reaction energy of the reaction in Eq. 17 obtained from the MM simulations, in kJ mol-1, $r_{\mathrm{H2S,model}}$, the rate of absorption of H_2S in the aqueous amine solvent in s^{-1}, A is in

mol kJ^{-1}, and B is dimensionless. We tried to further improve the strength of the correlation between $r_{\mathrm{H2S,model}}$ and ΔE_{H2S} by including the concentrations of H_2S and OH^- in Eq. 18 to obtain a relationship equivalent to that of CO_2 (Eq. 12). However, the inclusion of the concentrations did not lead to a stronger correlation and was therefore not included in the model of the absorption rate of H_2S. Full details are provided in the Supporting Information.

A and B are fitted to minimize the weighted RMSD (*wRMSD*) between the experimental rates and the model rates in Eq. 18. The weights are inversely proportional to the experimental error on the experimental rates of absorption. The energies of the reaction in Eq. 17 for all experimentally measured aqueous amine solvents (Table *1*) are given in the Supporting Information (Table T12). A set of only 10 values is used to fit *A* and B. It is not critical which values are chosen because of the excellent agreement in the fitting procedure. The experimental and calculated absorption rates of H_2S are shown in **Figure 3**. For $r_{\mathrm{H2S,model}}$ in s^{-1} in Eq. 18, we have *A*=0.1959 mol kJ^{-1} and B=–8.91. *RMSD* and *wRMSD* in **Figure 3** are evaluated using the entire set of values. This relative *RMSD* is equivalent to the relative *RMSD* value obtained in the case of the calculated CO_2 absorption rate [30].

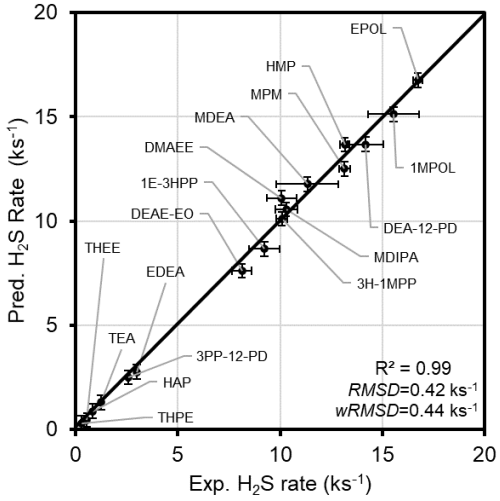

Figure 3. Computed and experimental rates of absorption of H_2S in aqueous ternary amine solvents (13% mol. amine, 87% mol. H_2O) at 323.15 K.

The previously derived model of CO_2 uptake rate is expressed in g L^{-1} min^{-1} [30] and not in s^{-1} as in the present study. In addition, we noted in Rozanska *et al*. [30] that the CO_2 kinetic model contains specific information related to the experimental protocol, which needs to be calibrated to the considered set of experimental data. The experimental protocol for measuring the CO_2 uptake rates is different in the present study and in the set of CO_2 data used previously [28]. The conversion of concentration from mol L^{-1} to fractional x is done using:

$$C = x\frac{\rho_s}{M_s} \qquad \text{Eq. 19}$$

where C is the concentration in mol L^{-1}, ρ_s the density of the solvent (Table S1), and M_s the molar mass of the solvent, which is $xM_a+(1-x)M_{H2O}$, where x=0.13 (for a 13%mol amine solvent), M_a the molar mass of the amine in g mol^{-1}, and M_{H2O}, the molar mass of H_2O in g mol^{-1} [51]. For ρ_s, we used the computed density (Supporting Information). The unit conversions from g CO_2 to mol CO_2 and from min^{-1} to s^{-1} must also be considered. After these unit conversions, the rates of CO_2 as obtained from molecular dynamics simulations using the previous model and data [30] were recalibrated to the present data set and the associated experimental apparatus and measurement conditions. Only a limited number of systems are needed for this recalibration, as mentioned in Rozanska *et al*. [30], using a simple linear relationship. The comparison of the selected calculated and experimental CO_2 absorption rates is shown in **Figure 4**.

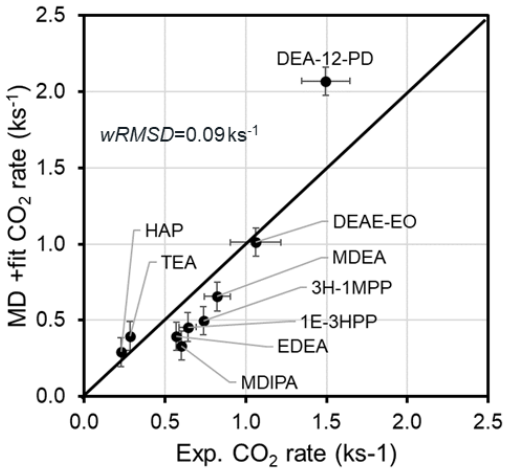

Figure 4. Computed and experimental rates of absorption of CO_2 in aqueous tertiary amine solvents (13% mol. amine, 87% mol. H_2O) at 323.15 K.

DISCUSSION

The model for the rate of absorption of CO_2 in aqueous amine solvent is based on Eq. 12 [30]. In the case of the rate of absorption of H_2S from Eq. 18, it is:

$$R_{\mathrm{MD}} = A(T) \times \exp\left(\frac{-\Delta G^{\neq}}{RT}\right) \qquad \text{Eq. 20}$$

namely, it is independent of the concentrations of H_2S and OH^-. It can also be expressed as:

$$R_{\mathrm{MD}} = A(T) \times \exp\left(\frac{-\Delta G^{\neq}}{RT}\right) P_{\mathrm{H_2S}} \qquad \text{Eq. 21}$$

as all rates were measured with the same H_2S partial pressure $P_{\mathrm{H_2S}}$. Eq. 21 is consistent with fast physisorption from gas to liquid phase and chemical reaction in the liquid phase, which is the case for H_2S compared to CO_2. It is also consistent with the fact that the absorption rate of H_2S increases with the partial pressure of H_2S, as described in previous empirical kinetic models [16].

As can be seen in **Figure 1**, the absorption rates of H_2S are approximately one order of magnitude greater than those of CO_2. Additional experimental measurements are needed to validate the kinetic model in Eq. 21 against that in Eq. 20 and the relationship between P_{H2S} and the rate of absorption of H_2S. However, the kinetic model for calculating the absorption rates of H_2S from the molecular dynamics simulation shows excellent agreement with the experimental values and can be readily used to analyze the relationship between the composition of the aqueous amine solvent and the absorption of H_2S and CO_2 and the H_2S/CO_2 absorption selectivity.

When H_2S/CO_2 selectivity and pK_a are included in **Figure 1**, some trends and features are observed from the experimental rates of absorption of CO_2 and H_2S (**Figure 5**).

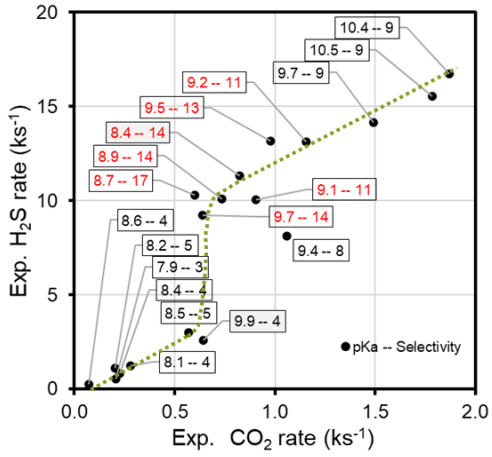

Figure 5. Experimental H_2S/CO_2 selectivity, amines pK_a, and rates of absorption of CO_2 and H_2S at T=323.15 K in the aqueous amine solvents (13%mol. amine, 87%mol. H_2O). The dotted line is a guide to the eye. The labels associated with each point in the graph are the pK_a and the H_2S/CO_2 selectivity (pK_a – Selectivity).

The rates of absorption of CO_2 and H_2S vary linearly with each other for most values and are related to some extent to the pK_a of the amine, with larger pK_a of the amine implying faster rates of absorption of H_2S and CO_2. However, when the CO_2 absorption rate is between 0.5 and 1.0 ks^{-1}, or when the pK_a is slightly above 8.5, a break occurs and the H_2S absorption rate becomes much faster. There are a few outliers in this simple analysis of the experimental rates.

The results shown in Figure 5 indicate that it is experimentally possible to tune the amines to control the H_2S/CO_2 absorption selectivity when aqueous tertiary alkanol amine solvents are considered.

In the case of the CO_2 absorption rate in aqueous amine solvents, the kinetic model we described in Rozanska et al. [30] was used to calculate the absorption rates of a set of 100 amines, which were then used to train a machine learning model [31]. This machine-learned model was based on the pK_a and topological descriptors of the amines. The rate of absorption of H_2S is likely to be sensitive to the structure of the amine. Therefore, we extended the molecular dynamics simulations to several additional amines to test the above hypotheses. Two sets of amines were selected from the 100 amines previously used to calculate CO_2 absorption rates. In the first set, the amines have a calculated CO_2 absorption rate between 0.5 and 1.0 ks^{-1} and a pK_a between 8.5 and 9.5. In addition, they are topologically like the selection of amines with high H_2S/CO_2 selectivity based on the Tanimoto's index [52] [53], namely MDEA, MDIPA, and 1E-3HPP. These criteria are empirical criteria from the experimental values (**Figure 5**). In the second set, the selected amines do not meet one or all the above criteria. The details of the 19 amines in the first and second sets are given in the Supporting Information (Tables S13, S14). The calculated and experimental CO_2 and H_2S uptake rates are shown in **Figure 6**. Most of the amines in the first set show H_2S/CO_2 selectivity equivalent to the experimental amines. The amines in the

second set also show lower rates of H_2S absorption. However, there are several outliers in both the first and second sets, suggesting that the above empirical rules for qualifying a highly selective solvent are likely to be incomplete. The empirical rules, together with the calculated rates of absorption of CO_2 and H_2S, provide a good basis for suggesting amines worthy of experimental testing (Set 1 in **Figure 6**).

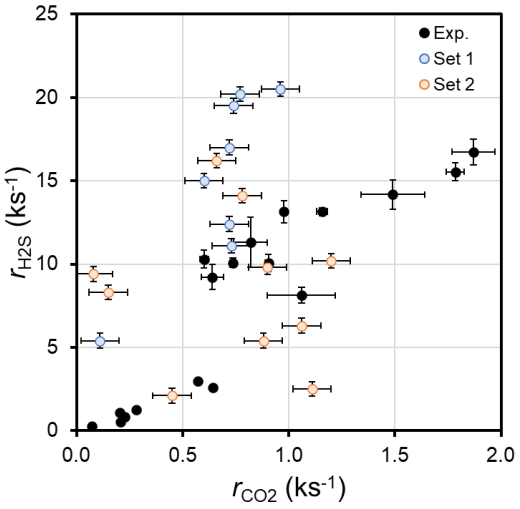

Figure 6. Experimental and computed rates of absorption of CO_2 and H_2S at T=323.15 K and x_{CO2} and x_{H2S}=0.5 in the aqueous amine solvents (13%mol. amine, 87%mol. H_2O). Set 1 and 2 designate sets of solvents that have a priori high and low H_2S/CO_2 absorption selectivity, respectively, following empirical rules as deduced from the experimental rates of absorption.

The combination of topological and chemical activity descriptors is relatively successful in predicting the absorption rates of H_2S, as evidenced by the data obtained for sets 1 and 2. In addition, Orlov *et al*. [31] recently derived a correlation model for the MD energies used to estimate the absorption rate of CO_2. Inspired by this work, we tested a correlation model using as the training set the MD reaction energies ΔE_{H2S} that are used in Eq. 18. To derive this correlation model, we used the quantitative structure-activity relationship (QSPR) tool as available in

MedeA [44]. Details of the correlation model can be found in the Supporting Information and the comparison between the MD and correlation ΔE_{H2S} values is shown in **Figure 7**.

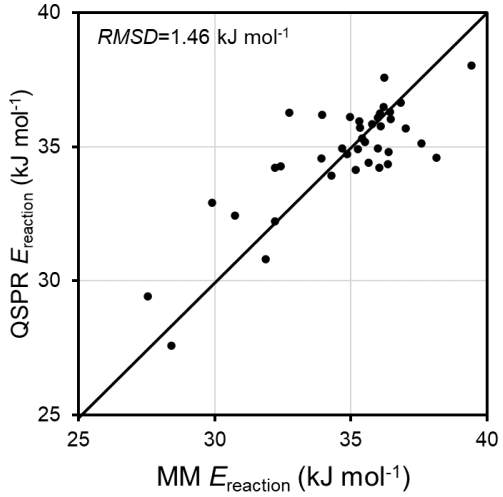

Figure 7. Comparison between the MM and QSPR reaction energies that are used to get the rate of absorption of H_2S at T=323.15 K and x_{H2S}=0.5 in the aqueous amine solvents (13%mol. amine, 87%mol. H_2O).

The *RMSD* between the MM and QSPR values is 1.46 kJ mol^{-1}, which is quite accurate. Only amine descriptors are used to obtain the correlation model. However, the accuracy of the QSPR model is not sufficient to derive a fully quantitative absorption rate of H_2S, as can be seen in **Figure 8**. The advantage of the QSPR model is that it can be used to screen a very large number of candidates and pre-select the most interesting amines. Unfortunately, due to its moderate accuracy, it cannot replace the MM values at this stage. However, QSPR also confirms that it is possible to estimate the rate of absorption of H_2S from a set of descriptors of the amine, as was done in the case of the rates of absorption of CO_2 [31].

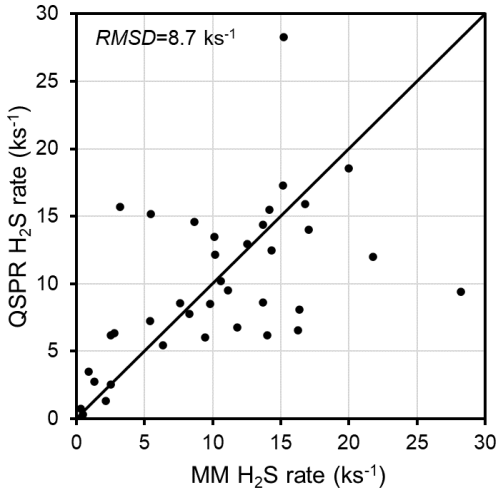

Figure 8. Comparison between the MM and QSPR rate of absorption of H_2S at T=323.15 K and x_{H2S}=0.5 in the aqueous amine solvents (13%mol. amine, 87%mol. H_2O).

CONCLUSIONS

We developed a protocol and apparatus to experimentally measure the absorption rates of CO_2 and H_2S. We then measured the absorption rates for a series of 18 aqueous alkanolamine solvents (13% molar amine). These experimental data represent the largest and most consistent set of data on simultaneous H_2S and CO_2 absorption rates in aqueous tertiary alkanolamine solvents to date. We observed that the absorption rates of CO_2 and H_2S vary linearly with each other for most values and are to some extent related to the pK_a of the amine. However, large deviations can also be observed. To better understand these deviations, we performed molecular dynamics simulations to derive a quantitatively very accurate model for the absorption rate of H_2S using a similar approach to that used to derive a model for the absorption rate of CO_2 [30]. With these CO_2 and H_2S models, it becomes possible to perform simulations to estimate the selectivity of a given aqueous amine solvent before experimental testing. From the analysis of the experimental CO_2 and H_2S absorption rates, we defined a set of simple rules for qualifying selective aqueous

amine solvents. We tested these rules by performing additional simulations and found that they are largely valid, although there are some outliers. Using the full set of simulation data obtained in this project, we developed a QSPR model of the absorption rate of H_2S, inspired by the correlation model derived in the case of the absorption rates of CO_2 [31]. This QSPR model is not as accurate as the MM simulation model, but it confirms that the absorption rates of H_2S in aqueous ternary alkanolamine solvents can be related to the amine through a set of chemical and topological descriptors of the amine. The merit of the QSPR model is that it can be applied to a very large number of amines, as was done in the case of the CO_2 model [31], thus allowing a screening of the amine database before performing MM simulations on the most promising candidates to verify their pertinence with higher accuracy.

Abbreviations

AGE: Acid Gas Enrichment
GC: Gas Chromatography
LNG: Liquefied Natural Gas
MM: Molecular Modelling
NPT: Number Pressure Temperature
PPPM: Particle-Particle-Particle-Mesh
QSPR: Quantitative Structure Property Relationship
RMSD : Root Mean Square Deviation
TCD: Thermal Conductivity Detectors
TGTU: TailGAs Treatment Unit

Supporting Information

The supporting Information contains more information on the experimental procedure and results, as well as on the molecular simulation based model and modelling results.

AUTHOR INFORMATION

Corresponding Authors

*Dr. Frédérick de Meyer. TotalEnergies S.E., OneTech, Gas & Low Carbon, Acid Gas Entity, CO_2 & Sustainability R&D Program, Paris, 92078 France

email: frederick.de-meyer@totalenergies.com.

Author Contributions

The manuscript was written through contributions of all authors. All authors have given approval to the final version of the manuscript.

Funding Sources

This work was supported by the CO_2 and Sustainability R&D Line from TotalEnergies.

REFERENCES

[1] R. Muñoz, L. Meier, I. Diaz et D. Jeison, «A review on the state-of-the-art of physical/chemical and biological technologies for biogas upgrading,» *Reviews in Environmental Science and Bio/Technology,* vol. 14, p. 727–759, 2015.

[2] Q. Sun, H. Li, J. Yan, L. Liu, Z. Yu et X. Yu, «Selection of appropriate biogas upgrading technology-a review of biogas cleaning, upgrading and utilisation,» *Renewable and Sustainable Energy Reviews,* vol. 51, p. 521-532, 2015.

[3] A. Kohl et R. Nielsen, Gas Purification, Oxford: Gulf Professional Publishing, 1997.

[4] F. de Meyer, R. Cadours et B. Poulain, «Development of a new ultra-selective solvent to reduce the cost to capture CO2 from a H2S-rich natural gas,» chez *Abu Dhabi International Petroleum Exhibition & Conference* , Abu Dhabi, 2022.

[5] F. de Meyer, C. Bignaud et B. Poulain, «Selective Electrochemical Regeneration of Aqueous Amine

Solutions to Capture CO2 and to Convert H2S into Hydrogen and Solid Sulfur,» *Applied Sciences,* vol. 11, n° 121, p. 9851, 2021.

[6] A. Pudi, M. Rezaei, V. Signorini, M. P. Andersson, M. G. Baschetti et S. S. Mansouri, «Hydrogen sulfide capture and removal technologies: A comprehensive review of recent developments and emerging trends,» *Separation and Purification Technology,* vol. 298, n° 1121448, 2022.

[7] A. A. Orlov, G. Marcou, D. Horvath, A. E. Cabodevilla, A. Varnek et F. de Meyer, «Computer-aided design of new physical solvents for hydrogen sulfide absorption,» *Industrial & Engineering Chemistry Research,* vol. 60, n° 123, p. 8588-8596, 2021.

[8] A. A. Orlov, D. Y. Demenko, C. Bignaud, A. Valtz, G. Marcou, D. Horvath, C. Coquelet, A. Varnek et F. de Meyer, «Chemoinformatics-Driven Design of New Physical Solvents for Selective CO2 Absorption,» *Environmental Science and Technology,* vol. 55, n° 122, p. 15542–15553, 2021.

[9] M. Shah, M. Tsapatsis et I. Siepmann, «Hydrogen Sulfide Capture: From Absorption in Polar Liquids to Oxide, Zeolite, and Metal–Organic Framework Adsorbents and Membranes» *Chemical Reviews,* vol. 117, n° 114, p. 9755–9803, 2017.

[10] G. Sartori et D. Savage, «Sterically hindered amines for carbon dioxide removal from gases,» *Industrial & Engineering Chemistry Fundamentals,* vol. 22, n° 12, p. 239–249, 1983.

[11] B. Mandal, A. Biswas et S. Bandyopadhyay, «Selective absorption of H2S from gas streams containing H2S and CO2 into aqueous solutions of N-methyldiethanolamine and 2-amino-2-methyl-1-propanol,» *Separation and Purification Technology,* vol. 35, n° 13, p. 191-202, 2004.

[12] J.-G. Lu, Y.-F. Zheng et D.-L. He, «Selective absorption of H2S from gas mixtures into aqueous solutions of blended amines of methyldiethanolamine and 2-tertiarybutylamino-2-ethoxyethanol in a packed column,» *Separation and Purification Technology,* vol. 52, n° 12, p. 209-217, 2006.

[13] L. Du, H. Li, L. Li, J. Xu et Y. Li, «Investigation of selective desulfurization performance of sterically hindered amines,» *Petroleum Science and Technology,* vol. 37, n° 11, p. 56-60, 2019.

[14] H. Li, L. Li, J. Xu et Y. Li, «Selective absorption of H2S from CO2 using sterically hindered amines at high pressure,» *Petroleum Science and Technology,* vol. 37, n° 115, p. 1825-1829, 2019.

[15] H. D. Frazier et A. L. Kohl, «Selective Absorption of Hydrogen Sulfide from Gas Streams,» *Ind. Eng. Chem.,* vol. 42, n° 111, p. 2288–2292, 1950.

[16] W.-C. Yu et G. Astarita, «Selective absorption of hydrogen sulphide in tertiary amine solutions,» *Chemical Engineering Science,* vol. 42, n° 13, p. 419-424, 1987.

[17] R. Giesen, «Mathematische Modellierung des MDEA-Absorptionsprozesses,» RWTH Aachen University, Aachen, 2004.

[18] G. F. Froment, K. B. Bischoff et J. De wilde, Chemical Reactor Analysis and Design, 3rd Edition,

Hoboken: John Wiley & Sons, 2011.

[19] W. G. Whitman, «The two film theory of gas absorption,» *International Journal of Heat and Mass Transfer,* vol. 5, n° 15, p. 429-433, 1962.

[20] Z. Qian, L.-B. Xu, Z.-H. Li, H. Li et K. Guo, «Selective Absorption of H2S from a Gas Mixture with CO2 by Aqueous N-Methyldiethanolamine in a Rotating Packed Bed,» *Industrial & Engineering Chemistry Research,* vol. 49, n° 113, p. 6196–6203, 2010.

[21] W. Jiao, P. Yang, G. Qi et Y. Liu, «Selective absorption of H2S with High CO2 concentration in mixture in a rotating packed bed,» *Chemical Engineering and Processing - Process Intensification,* vol. 129, p. 142-147, 2018.

[22] R. Wanderley, Y. Yuan, G. Rochelle et H. Knuutila, «CO2 solubility and mass transfer in water-lean solvents,» *Chemical Engineering Science,* vol. 202, p. 403-416, 2019.

[23] U. Shoukat, D. Pinto et H. Knuutila, «Study of Various Aqueous and Non-Aqueous Amine Blends for Hydrogen Sulfide Removal from Natural Gas,» *Processes,* vol. 7, n° 13, p. 160, 2019.

[24] K. Gonzalez, L. Boyer, D. Almoucachar, B. Poulain, E. Cloarec, C. Magnon et F. de Meyer, «CO2 and H2S absorption in aqueous MDEA with ethylene glycol: Electrolyte NRTL, rate-based process model and pilot plant experimental validation,» *Chemical Engineering Journal,* 2022.

[25] H.-J. Xu, C.-F. Zhang et Z.-S. Zheng, «Solubility of Hydrogen Sulfide and Carbon Dioxide in a Solution of Methyldiethanolamine Mixed with Ethylene Glycol,» *Industrial & Engineering Chemistry Research,* vol. 41, n° 124, p. 6175–6180, 2002.

[26] T. Carey, J. Hermes et G. Rochelle, «A model of acid gas absorption/stripping using methyldiethanolamine with added acid,» *Gas Separation & Purification,* vol. 5, n° 12, p. 95-109, 1991.

[27] I. Bernhardsen et H. Knuutila, «A review of potential amine solvents for CO2 absorption process: Absorption capacity, cyclic capacity and pKa,» *International Journal of Greenhouse Gas Control,* vol. 61, p. 27-48, 2017.

[28] F. A. Chowdhury, H. Okabe, S. Shimizu, M. Onoda et Y. Fujioka, «Development of novel tertiary amine absorbents for CO2 capture,» *Energy Procedia,* vol. 1, n° 11, p. 1241-1248, 2009.

[29] A. Hartono, S. J. Vevelstad, A. Ciftja et H. K. Knuutila, «Screening of strong bicarbonate forming solvents for CO2 capture,» *Int. J. Greenh. Gas Control.,* vol. 58, p. 201-211, 2017.

[30] X. Rozanska, E. Wimmer et F. de Meyer, «Quantitative Kinetic Model of CO2 Absorption in Aqueous Tertiary Amine Solvents,» *Journal of Chemical Information and Modeling,* vol. 61, n° 14, p. 1814–1824, 2021.

[31] A. A. Orlov, A. Valtz, C. Coquelet, X. Rozanska, E. Wimmer, G. Marcou, D. Horvath, B. Poulain, A. Varnek et F. de Meyer, «Computational screening methodology identifies effective solvents for CO2

capture,» *Communications Chemistry,* vol. 5, n° 37, 2022.

[32] R. Cadours, C. Bouallou, A. Gaunand et D. Richon, «Kinetics of CO2 Desorption from Highly Concentrated and CO2-Loaded Methyldiethanolamine Aqueous Solutions in the Range 312−383 K,» *Industrial & Engineering Chemistry Research,* vol. 36, n° 112, p. 5384–5391, 1997.

[33] C. Coquelet , A. Valtz et P. Théveneau, «Experimental Determination of Thermophysical Properties of Working Fluids for ORC Applications,» chez *Organic Rankine Cycles for Waste Heat Recovery-Analysis and Applications*, IntechOpen, 2019.

[34] 0. Kunz et W. Wagner, «The GERG-2008 Wide-Range Equation of State for Natural Gases and Other Mixtures: An Expansion of GERG-2004,» *Journal of Chemical & Engineering Data,* vol. 57, n° 111, p. 3032–3091, 2012.

[35] E. W. Lemmon, M. L. Huber et M. O. McLinden, «NIST Standard Reference Database 23: Reference Fluid Thermodynamic and Transport Properties-REFPROP, Version 9.1,» Natl Std. Ref. Data Series , 2013.

[36] K. R. Putta, F. A. Tobiesen, H. F. Svendsen et H. K. Knuutila, «Applicability of enhancement factor models for CO2 absorption into aqueous MEA solutions,» *Applied Energy,* vol. 206, p. 765-783, 2017.

[37] R. B. Bird, W. E. Stewart et E. N. Lightfoot, Transport Phenomena, New York: John Wiley and Sons, 1960.

[38] M. G. Evans et M. Polanyi, «Inertia and driving force of chemical reactions,» *Transactions of the Faraday Society,* vol. 34, p. 11-24, 1938.

[39] M. P. Allen et D. J. Tildesley, Computer Simulation of Liquids, New York: Oxford University Press, 1987.

[40] S. Plimpton, «Fast parallel algorithms for short-range molecular dynamics,» *Journal of computational physics,* vol. 117, n° 11, p. 1-19, 1995.

[41] H. Sun, S. J. Mumby, J. R. Maple et A. T. Hagler, «An ab initio CFF93 all-atom force field for polycarbonates,» *Journal of the American Chemical Society,* vol. 116, n° 17, p. 2978-2987, 1994.

[42] P. Ungerer, D. Rigby, B. Leblanc et M. Yiannourakou, «Sensitivity of the aggregation behaviour of asphaltenes to molecular weight and structure using molecular dynamics,» *Molecular Simulation,* vol. 40, n° 11-3, p. 115-122, 2014.

[43] X. Rozanska, P. Ungerer, B. Leblanc, P. Saxe et E. Wimmer, «Automatic and Systematic Atomistic Simulations in the MedeA® Software Environment: Application to EU-REACH,» *Oil & Gas Science and Technology–Revue d'IFP Energies nouvelles,* vol. 70, n° 13, p. 405-417, 2015.

[44] MedeA, «MedeA: Materials Exploration and Design Analysis. Copyright © 1998-2023 Materials Design, Inc. Version 3.1.,» 2023.

[45] B. A. Luty, M. E. Davis, I. G. Tironi et W. F. Van Gunsteren, «A comparison of particle-particle, particle-mesh and Ewald methods for calculating electrostatic interactions in periodic molecular systems,» *Molecular Simulation,* vol. 14, n° 11, p. 11-20, 1994.

[46] X. Daura, A. E. Mark et W. F. Van Gunsteren, «Parametrization of aliphatic CHn united atoms of GROMOS96 force field,» *Journal of computational chemistry,* vol. 19, n° 15, p. 535-547, 1998.

[47] D. J. Evans et B. L. Holian, «The nose–hoover thermostat,» *The Journal of chemical physics,* vol. 83, n° 18, p. 4069-4074, 1985.

[48] D. Frenkel et B. Smit, Understanding molecular simulation: from algorithms to applications, Elsevier, 2001.

[49] K. Mansouri, C. M. Grulke, R. S. Judson et A. J. Williams, «OPERA models for predicting physicochemical properties and environmental fate endpoints,» *Journal of cheminformatics,* vol. 10, n° 11, p. 1-19, 2018.

[50] C. Nieto-Draghi, G. Fayet, B. Creton, X. Rozanska, P. Rotureau, J.-C. de Hemptinne, P. Ungerer, B. Rousseau et C. Adamo, «A General Guidebook for the Theoretical Prediction of Physicochemical Properties of Chemicals for Regulatory Purposes,» *Chem. Rev.,* vol. 115, n° 124, p. 13093–13164, 2015.

[51] R. Sander, «Compilation of Henry's law constants (version 4.0) for water as solvent,» *Atmospheric Chemistry and Physics,* vol. 15, n° 18, p. 4399-4981, 2015.

[52] D. R. Flower, «On the properties of bit string-based measures of chemical similarity,» *Journal of chemical information and computer sciences,* vol. 38, n° 13, p. 379-386, 1998.

[53] N. M. O'Boyle, M. Banck, C. A. James, C. Morley, T. Vandermeersch et G. R. Hutchison, «Open Babel: An open chemical toolbox,» *Journal of cheminformatics,* vol. 3, n° 11, p. 1-14, 2011.